

---

# Oxidation Behavior of YAG-Al<sub>2</sub>O<sub>3</sub> Coatings Toughened by Pt Nano-Particles

Peng Wang<sup>\*</sup>, Yu Xinmin, Liu Junpeng, Zuo Hongjun, Huo Pengfei

Research Institute of Aerospace Special Materials and Processing Technology, Beijing, China

**Email address:**

18810351480@163.com (Peng Wang)

<sup>\*</sup>Corresponding author

**To cite this article:**

Peng Wang, Yu Xinmin, Liu Junpeng, Zuo Hongjun, Huo Pengfei. Oxidation Behavior of YAG-Al<sub>2</sub>O<sub>3</sub> Coatings Toughened by Pt Nano-Particles. *Nanoscience and Nanometrology*. Vol. 4, No. 1, 2018, pp. 16-22. doi: 10.11648/j.nsnm.20180401.13

**Received:** July 20, 2018; **Accepted:** August 3, 2018; **Published:** September 1, 2018

---

**Abstract:** YAG (Y<sub>3</sub>Al<sub>5</sub>O<sub>12</sub>)-Al<sub>2</sub>O<sub>3</sub>-Pt composite TBCs have been prepared on Ni-based superalloy (0.1% C, 12% Co, 6.5% Cr, 6.2% Al, 5% W, 1% Mo, 1.5% Hf, 6.5% Ta, 0.01% B, balance Ni, wt.%) by cathode plasma electrolytic deposition (CPED). As polyethylene glycol (PEG) is added in solution, the spark ignition current density is reduced significantly, and CPED would be a promising technique to deposit the uniform coatings on large-sized cathode. The cyclic oxidation tests at 1100°C reveal that the high temperature oxidation resistance of such TBCs are significantly improved by dispersing Pt particles. These excellent performances can be attributed to the effects: the low porosity of coating can inhibit further oxidation of alloy substrate, the toughening role of Pt particles and the stress relaxation caused by the deformation in the porous structure can improve the mechanical properties remarkably. The spallation resistance of YAG-Al<sub>2</sub>O<sub>3</sub>-Pt composite coating can be significant improved by using the following two method: one is adding PEG 20000 to the solution during the CPED process; the other is using Pt particle to toughen the coating. In addition, such YAG-Al<sub>2</sub>O<sub>3</sub>-Pt composite coatings possess quite well thermal insulation owing to the thermal insulation capability of YAG and the structure of vertical block micropores.

**Keywords:** Cathode Plasma Electrolytic Deposition, YAG-Al<sub>2</sub>O<sub>3</sub>-Pt Composite Coatings, Thermal Barrier Coatings

---

## 1. Introduction

Thermal barrier coatings (TBCs) have been widely used in the gas turbine engines to protect the metal components performing in high temperature, oxidative, and hot corrosive environment [1, 2]. The common TBC system consists of a ceramic top coat layer, a metallic bond coat layer, thermal grown oxide (TGO) layer and the alloy substrate [3]. The top coat is commonly composed of Yttria-stabilized zirconia ZrO<sub>2</sub>-8%Y<sub>2</sub>O<sub>3</sub> (8YSZ) [4], because of its low thermal conductivity and relatively high thermal expansion coefficient. The bond coat layer is made of MCrAlY or aluminides of Ni and Pt [5], which can provide good adhesion and strong oxidation protection for the superalloy substrate [6]. TGO layer forms at the top/bond coat interface during engine service. Such TGO has low oxygen diffusivity and can inhibit further oxidation of the bond coat. But the thermal stress caused by the mismatch of thermal expansion between top coat and bond coat can lead to the cracking and spallation at the TGO layer, which is the key

factor in the failure of TBCs [7]. During service at high temperature, the interdiffusion between the metallic bond coat and superalloy substrate cannot be avoided, it would reduce the mechanical properties of turbine blade. Furthermore, YSZ is not stable over the 1250°C, so the application of YSZ top coat at higher temperature is difficult [8].

In order to solve above problems, different materials with higher operating temperature have studied recently, such as YAG, La<sub>2</sub>Zr<sub>2</sub>O<sub>7</sub> and LaTi<sub>2</sub>Al<sub>9</sub>O<sub>19</sub>. Among these above materials, YAG (Y<sub>3</sub>Al<sub>5</sub>O<sub>12</sub>) is considered to be a promising top coat material. YAG is composed of Al<sub>2</sub>O<sub>3</sub> and Y<sub>2</sub>O<sub>3</sub>, which possesses not only good oxidation resistance, but also low thermal conductivity. In addition, YAG has a good thermal stability up to the melting point (2243 K) [9]. However, the thermal expansion coefficient of YAG is so low that could lead to the cracking and spallation of the coating. Therefore, toughening the YAG coating is the key factor to solve this problem. It has been proved that composite structure is an effective way to improve the durability of materials, such as mixture composite, which has better mechanical properties than that with a single phase structure [10,

11]. Alumina ( $\text{Al}_2\text{O}_3$ ) possesses a very low oxygen diffusivity and high hardness [12]. So, the combination of YAG and  $\text{Al}_2\text{O}_3$  will contribute to improve the mechanical and oxidation resistance of the coating. Besides, in order to improve the spallation resistance of  $\text{Al}_2\text{O}_3$  coating, the Au particles dispersed  $\text{Al}_2\text{O}_3$  composite coating was prepared by Xiaoxu Ma et al. [13]. And this work provides a possibility for developing the single layer TBCs. Thus, the YAG- $\text{Al}_2\text{O}_3$ -Pt composite TBC has been proposed by the research group.

Nowadays the technologies to prepare the TBCs, which have been applied in industry, are plasma spraying (PS) [14] and electron beam physical vapor deposition (EB-PVD) [15]. TBCs deposited by plasma spraying have good adhesion with substrate, but the device is rather costly and the coating has many defects which will decrease the lifetime of coating greatly. In order to improve the shortage of PS, another technique (EB-PVD) started to be researched from 1970s. The coatings deposited by EB-PVD possess columnar crystal structure. Thus, the lifetime of coating can be increased due to the stress relaxation caused by the deformation of this structure. However, the thermal conductivity of the coating with columnar crystal structure is very high. Moreover, the preparation cost is high and EB-PVD cannot be applied on complex shapes of work piece. So a new deposition technology of TBCs should be developed.

Cathode plasma electrolytic deposition (CPED) is a hybrid of conventional electrolysis and plasma process, which has been studied for decades [16]. Yang X. Z. et al. [17] has prepared a thick 8YSZ coating on FeCrAl alloy by cathodic micro-arc electrodeposition. And later this technique was improved and termed as CPED. After then researchers [18, 19] have prepared  $\text{Al}_2\text{O}_3$  TBC by CPED, and the coating is continuous and combines with the substrate well.

Porous YAG- $\text{Al}_2\text{O}_3$  composite TBCs dispersed with Pt particles were prepared on superalloy by CPED. The composition, structure and property of such TBCs were investigated. The kinetic of electrode processes and the formation mechanism of TBCs were investigated by testing the current density-voltage curve ( $i_c$ - $V$  curve) of the CPED processes. And the mechanisms on the toughening role of Pt particles were discussed. It is expected that this study could promote the development of TBCs with novel structures.

## 2. Method

### 2.1. Coating Preparation

The schematic view of CPED device for preparing YAG- $\text{Al}_2\text{O}_3$  composite coatings (YA), YAG- $\text{Al}_2\text{O}_3$  composite coatings dispersed with Pt particles (YAPt) and measuring  $i_c$ - $V$  curves is shown in Figure 1. A platinum electrode was worked as anode with a dimension of 120mm×50mm×0.3mm. The samples of Ni-based superalloy (0.1% C, 12% Co, 6.5% Cr, 6.2% Al, 5% W, 1% Mo, 1.5% Hf, 6.5% Ta, 0.01% B, balance Ni, wt.%) were used as cathode 15 mm×10 mm×2 mm and the surfaces of samples were ground #1500 grit SiC papers, ultrasonically cleaned in ethanol. A pulsed electrical

power supply (TN-KGZ01) was connected in the electrolytic bath. The CPED process was carried out in the aqueous solutions of  $\text{Al}(\text{NO}_3)_3$ ,  $\text{Y}(\text{NO}_3)_3$  and PEG (20 g/L) with 0, 0.08, 0.16, 0.24 g/L  $\text{H}_2\text{PtCl}_6 \cdot 6\text{H}_2\text{O}$  respectively. The molar ratio of  $\text{Al}^{3+}/\text{Y}^{3+}$  is 65/35 and the total concentration is 1 mol/L. The applied voltage was changed from 120 to 170 V step by step. The frequency was 500 Hz. The duty ratio was 60%, and the depositing time was kept at 1 h.

In addition,  $i_c$ - $V$  curves were measured in solutions without and with 20 g/L PEG respectively, and the bath voltage (under the direct-current condition) was increased from 0 to 135 V at a rate of 1 V/s, meanwhile the cathode current density  $i_c$  and bath voltage  $V$  were recorded by a computer.

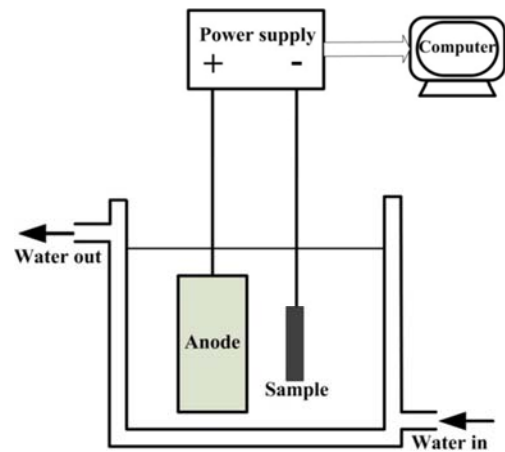


Figure 1. The schematic view of the CPED device.

### 2.2. Coating Characterization

The morphologies of YA coatings with different Pt content were investigated by scanning electron microscope (SEM, JMS-6480A) with an energy-dispersive spectroscopy (EDS) system. The phase structures were detected by X-ray diffraction analysis (XRD, PW 3710, Philips) at room temperature using nickel filtered  $\text{Cu K}\alpha$  radiation in the  $2\theta$  range of 10-90° with a step size of 0.02°.

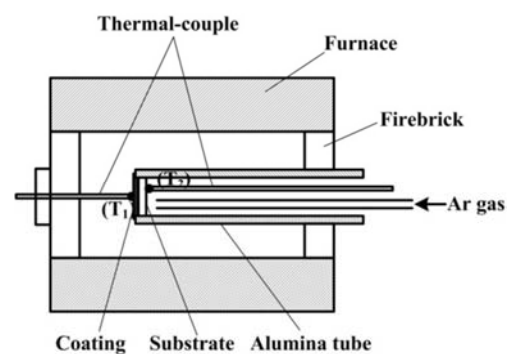


Figure 2. Schematic diagram of the device of thermal insulation capability test.

High temperature cyclic oxidation tests were carried out to investigate the kinetics of oxidation and spallation resistance of coatings in air furnace at 1100°C for 200 h. After a certain oxidation period of 10 h, samples were taken out and air

cooling to the room temperature, the mass gain (sample + spalling oxide + crucible) and spallation mass (spalling oxide + crucible) were weighed by the analytical balance (BT 25S, Sartorius) respectively. Then put the samples back to the furnace, and repeated this cycle 20 times.

The thermal insulation capability tests were carried out in the device as shown in Figure 2. Two k-typed thermal-couples were applied as sensors to record the temperatures on the coating surface ( $T_1$ ) and on the uncoated alloy surface ( $T_2$ ) respectively. Ar gas was used to cool the substrate alloy with a flow rate of 5 liters per minute. The thermal insulation capability was evaluated by the temperature drop  $\Delta T = T_1 - T_2$ .

### 3. Result

#### 3.1. Morphologies of the Prepared Coatings

Figure 3 shows the  $i_c$ - $V$  curves of CPED processes of

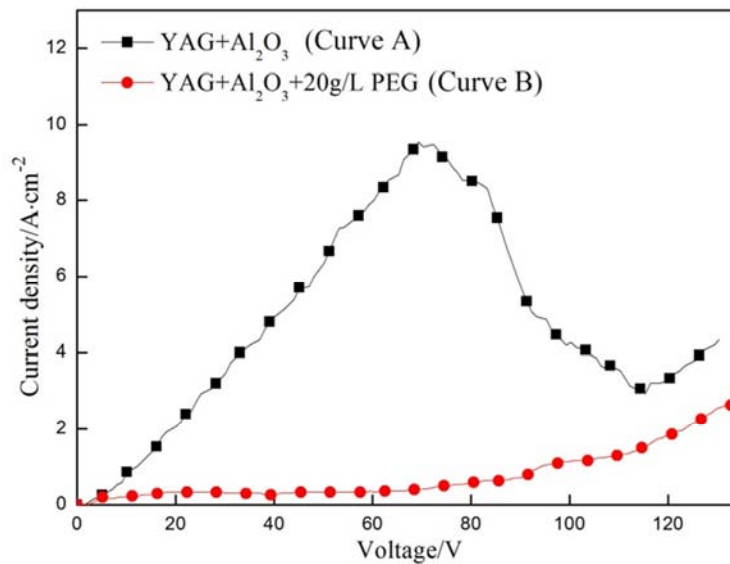


Figure 3. The current density-voltage curves without and with PEG in the solution.

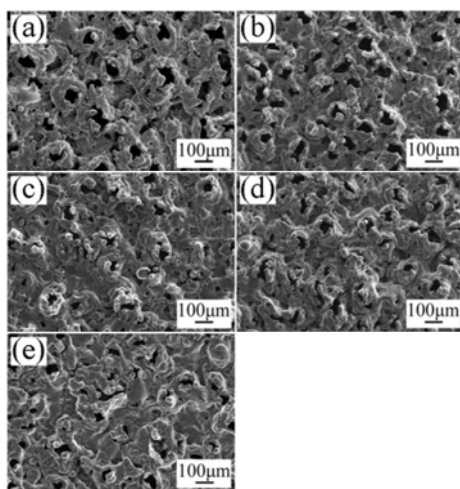


Figure 4. SEM surface images of composite coatings prepared in solutions containing different concentrations of PEG and  $\text{H}_2\text{PtCl}_6 \cdot 6\text{H}_2\text{O}$ : (a) 0 g/L, 0 g/L; (b) 20 g/L, 0 g/L; (c) 20 g/L, 0.2 g/L (d) 20 g/L, 0.4 g/L and (e) 20 g/L, 0.6 g/L.

different samples measured in solution without and with PEG. It can be seen that there is a tremendous influence on the  $i_c$ - $V$  curve, and the current density is decreased significantly by adding PEG in solution. Compared Figure 4a with Figure 4b, it can be seen that the micro-pores of coating become larger by adding PEG. As adding  $\text{H}_2\text{PtCl}_6$  in the solution, the micro-pores of coating start to become small, as shown in Figure 4b-e, and the sizes of pores become small as the concentration of  $\text{H}_2\text{PtCl}_6$  increasing. Figure 5 shows the cross section SEM images of the YAG- $\text{Al}_2\text{O}_3$  composite coatings on the Ni-based super alloy. It can be seen that the coating is rather uniform and the total thickness of the coating is about 200  $\mu\text{m}$ . It has a new micro-structure: the outer layer is porous, while the inner layer is compact. Figure 6 shows the morphology of Pt particle formed in the coating and EDS analysis result which can prove that the Pt particles exist in the coatings.

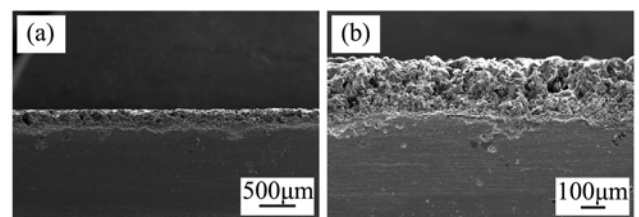


Figure 5. SEM image of cross-section morphologies of the composite coatings: (a) the image of 30 times; (b) the image of 100 times.

Figure 7 shows the XRD spectra patterns of the samples coated with YAG- $\text{Al}_2\text{O}_3$  composite coating before and after cyclic oxidation. It can be seen that YAG and  $\alpha$ - $\text{Al}_2\text{O}_3$  phase have been formed in the composite coatings. After cyclic oxidation at 1100°C for 200 h, there is no phase transformation in the coatings, which proves that the composite coatings are stable at high temperature.

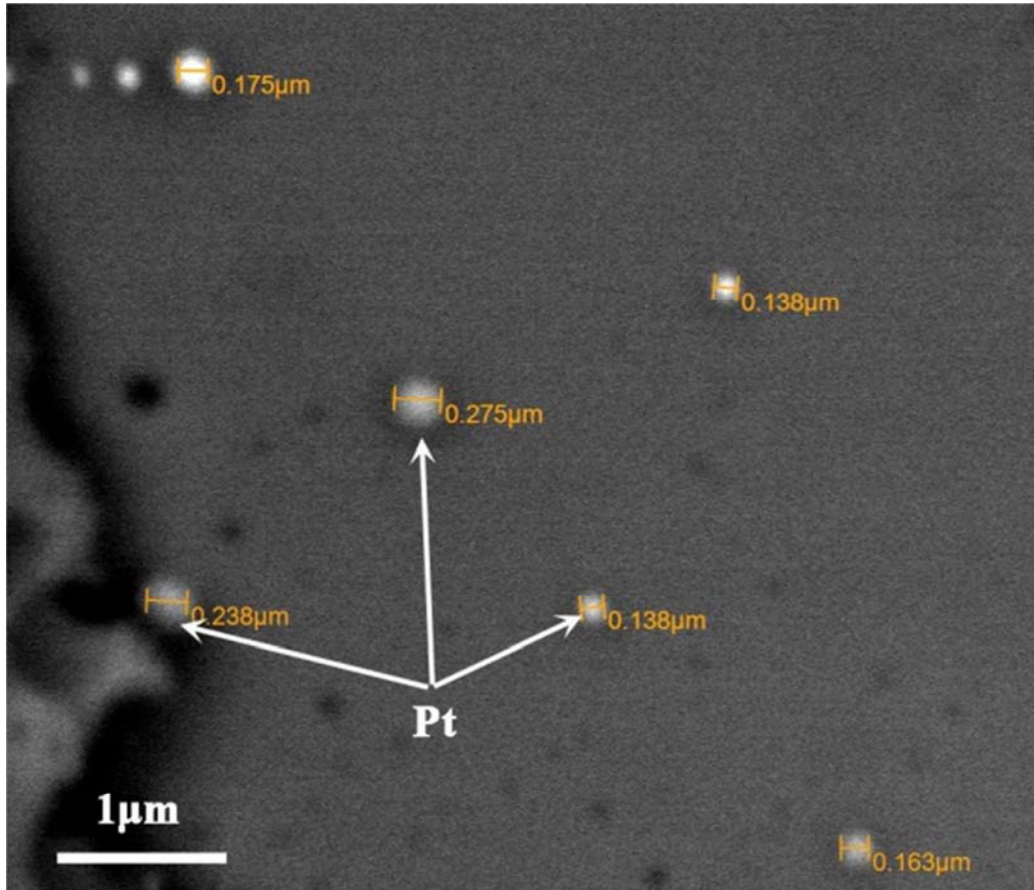


Figure 6. Back scattered-electron SEM surface image of coating.

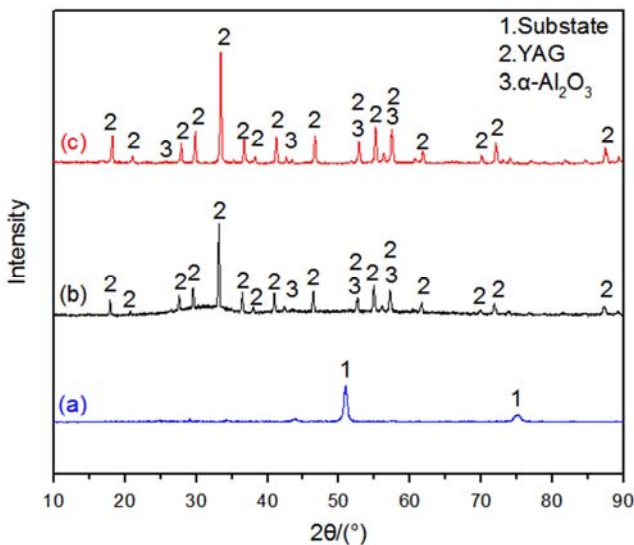


Figure 7. XRD spectra patterns of samples coated with YAG- $\text{Al}_2\text{O}_3$  composite coating: (a) blank; (b) YAG- $\text{Al}_2\text{O}_3$  composite coating; (c) YAG- $\text{Al}_2\text{O}_3$  composite coating after cyclic oxidation.

### 3.2. High-Temperature Cyclic Oxidation Kinetics

Figure 8 shows the oxidation kinetic curves of different samples at  $1100^\circ\text{C}$  for 200 h. It can be seen that after 200 h cyclic oxidation, the weight gain and spallation of the bare

Ni-based superalloy were up to  $1.37 \text{ mg/cm}^2$  and  $1.25 \text{ mg/cm}^2$ , owing to the serious oxidation of the substrate and excessive internal stresses. The coating prepared in the solution of  $\text{Al}(\text{NO}_3)_3 + \text{Y}(\text{NO}_3)_3$  has peeled after cyclic oxidation for 50 h, while the coating prepared in the solution of  $\text{Al}(\text{NO}_3)_3 + \text{Y}(\text{NO}_3)_3 + \text{PEG}(20 \text{ g/L})$  is for 170 h. It prove that adding PEG in the solution can improve the oxidation and spallation resistant of the coating. Compared the line 3-6 in Figure 8a-b, it shows that the high temperature oxidation and spallation resistance of YAG- $\text{Al}_2\text{O}_3$  composite coatings have been significantly improved with the Pt particles.

Figure 9 shows SEM images of the morphologies of different samples after cyclic oxidation. It can be seen from the Figure 9a and e that, a loose and thick oxide scale has been formed on the bare Ni-base super alloy during cyclic oxidation. These loose structures would provide rapid inward oxygen diffusion path. Figure 9b-d has shown the morphologies of the coatings after oxidation. It can be seen that the coating become compact and the micropores become small. It indicated that the coatings have been sintered and the micropores could relax the thermal stresses during the cyclic oxidation. Figure 9f shows the cross-section of the coating. It can be seen that the coating is still continuous and the scale of alloy substrate is thin. This has demonstrated that the coating has a good oxidation and spallation resistance.

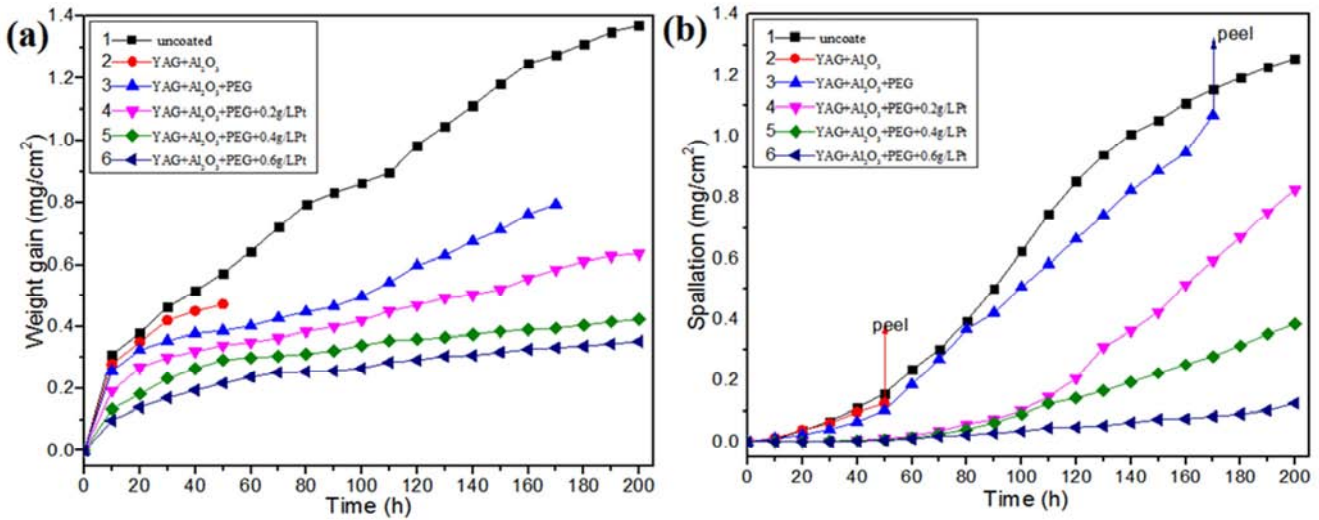


Figure 8. Oxidation kinetic curves of different sample at 1100°C for 200 h: (a) weight gain versus time; (b) spallation versus time.

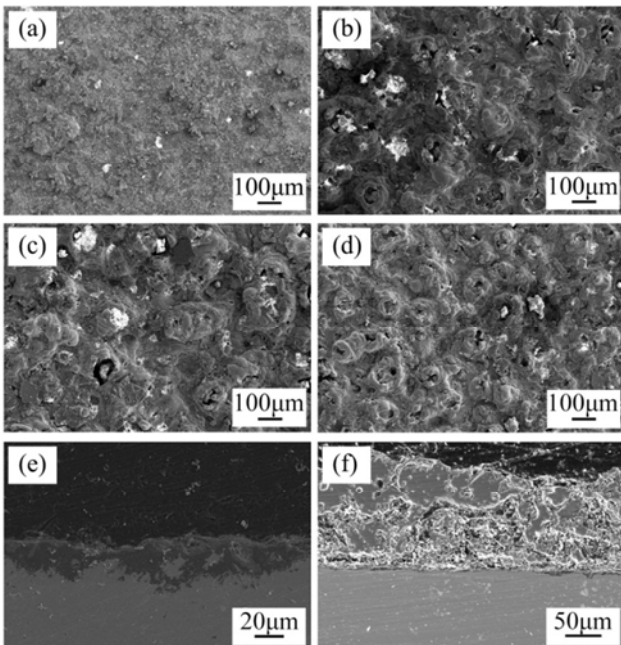


Figure 9. The morphology of the blank sample and the composite coating after cyclic oxidation: (a) surface of blank sample; (b) surface of the coating YAG+ $\text{Al}_2\text{O}_3$ + PEG +0.2 g/L Pt; (c) surface of the coating YAG+ $\text{Al}_2\text{O}_3$ + PEG +0.4 g/L Pt; (d) surface of the coating YAG+ $\text{Al}_2\text{O}_3$ + PEG +0.6 g/L Pt; (e) cross-section of blank sample; (f) cross-section of the composite coating 0.6 g/L Pt.

### 3.3. Thermal Insulation Capability

Figure 10 shows the thermal insulation capability of the YAG- $\text{Al}_2\text{O}_3$ -Pt composite coating with the Ar gas flow rate of 5 L/min. It can be seen that this composite coating has a good thermal insulation capability. The biggest temperature difference is 200°C. This great thermal insulation capability can be attributed to the thermal insulation capability of YAG and the structure of vertical block micropores.

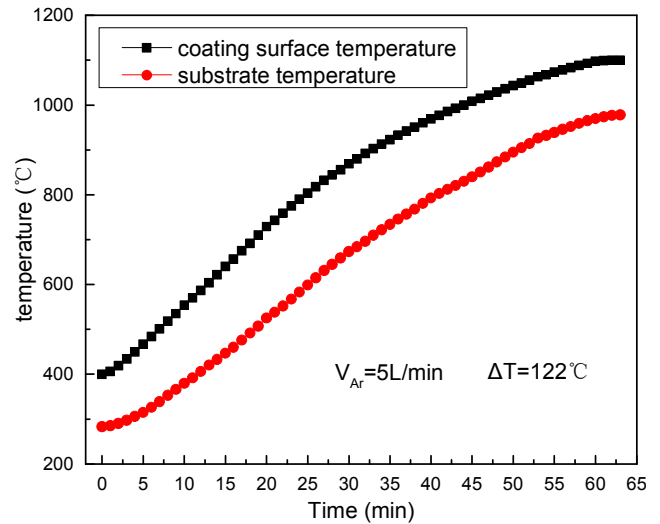


Figure 10. Thermal insulation capability of the composite coating with Ar gas flow rate of 5 L/min from 400°C to 1100°C.

## 4. Discussion

The experiment results demonstrated that the YAG- $\text{Al}_2\text{O}_3$  composite coating exhibited excellent high-temperature oxidation and spallation after cyclic oxidation. And the porous coating prepared by CPED has well property of thermal insulation. The mechanism accounting for these excellent properties are discussed as followed.

### 4.1. Mechanism of the Improvement of the High-temperature Oxidation Resistance of the YAG- $\text{Al}_2\text{O}_3$ Composite Coating Dispersed with Pt Particle

In this study, YAG- $\text{Al}_2\text{O}_3$  composite coating has been deposited on the Ni-based superalloy. Since no interdiffusion can take place between the ceramic coating and alloy substrate, the outward diffusion of the alloy elements has been inhibited effectively. Thus, the controlling step in the oxidation of

substrate is inward diffusion of oxygen. As the oxygen diffusion coefficient of YAG is about 10 orders of magnitude lower than  $ZrO_2$ , which can demonstrate that YAG is oxygen impermeable. And it is widely known that  $\alpha-Al_2O_3$  is one of the ideal oxygen diffusion barrier materials. So YAG- $Al_2O_3$  composite coating itself has a very good oxidation resistance. At the same time, the coating is rather thick and the inner layer is compact, the diffusion rate of  $O^{2-}$  is very low. Therefore the partial press of oxygen at the interface of coating/substrate is very low, which is not enough to form oxide of Ni and Cr. According to Wagner [20, 21], the low partial press of oxygen would promote the selective oxidation of the Al in high temperature, just as shown in Figure 10. And Al would be oxidized into  $\alpha-Al_2O_3$ , which can efficiently retard further oxidation of substrate.

#### 4.2. Mechanisms of the Improvement of the Special Mechanical Properties of the YAG- $Al_2O_3$ Composite Coating Dispersed with Pt Particle

From the high temperature oxidation experiment results as shown in Figure 7, the YAG- $Al_2O_3$  composite coating did not show a good oxidation resistance, due to the premature spallation. However, the YAG- $Al_2O_3$  composite coating dispersed with Pt can remarkably improve the spallation resistance of the Ni-based superalloy after 200 h thermal cycling and the spallation of the coating significantly improved with the increase of the amount of Pt. The mechanisms are discussed as follows.

It is known that the high temperature oxidation resistance of the protective coatings is mainly determined by their spallation and crack resistance. And the spallation and crack of the coating are often caused by thermal stresses, which arise from the differential thermal expansion between alloy substrate and surface coating. The composite coating prepared by CPED has a special structure that the inner layer is compact and the outer layer is porous. As the spalling of a compressively stressed coating will occur when the elastic strain energy stored in the intact scale exceeds the fracture,  $G_c$ , of the interface. As analysed by Evan, the criterion for failure can be given as following equation:

$$\frac{(1-\nu)\sigma^2 h}{E} > G_c \quad (1)$$

Where the  $\nu$ ,  $\sigma$ ,  $h$ ,  $E$  denote the Poisson's ratio, stress, thickness and elastic modulus of the coating. As the Poisson's ratio, thickness and elastic modulus of the coating is constant, according to Eq. (1), there are two ways to avoid coating spallation: one is decreasing the stress ( $\sigma$ ), the other is increasing the fracture resistance ( $G_c$ ).

During the cyclic oxidation, the stresses arise from different thermal expansion between the alloy substrate and the surface coating. As the thermal expansion of the ceramic is smaller than that of alloy substrate, so that the thermal stress ( $\sigma$ ) will develop in coating during cooling. According to Timoshenkou, the thermal stress can be given as the following Equation:

$$\sigma = \frac{-E(\alpha_{\text{coating}} - \alpha_M)\Delta T}{1-\nu} \quad (2)$$

Where  $E$  is the elastic modulus of the coating,  $\nu$  is the Poisson's ratio of the coating (the same below),  $\alpha_{\text{coating}}$  and  $\alpha_M$  are the linear thermal expansion coefficients for the coating and alloy substrate and  $\Delta T$  is the change in temperature. It can be seen from Eq. (2) that the thermal stress has linear relationship with the difference of temperature and coefficient of thermal expansion (CTE). From table. 1, it can be seen that the CTE of the three materials in the coating is similar and smaller than that of alloy substrate. Thus, it is difficult to avoid coating spallation by decreasing the  $\Delta CTE$  ( $\alpha_{\text{coating}} - \alpha_M$ ) in this study.

Table 1. The CTE of materials in the sample.

Material	YAG	$Al_2O_3$	Pt	Substrate
CTE	$6.9 \times 10^{-6} K^{-1}$	$7.8 \times 10^{-6} K^{-1}$	$9 \times 10^{-6} K^{-1}$	$13 \times 10^{-6} K^{-1}$

Therefore, the other way which is increasing the fracture resistance ( $G_c$ ) should be the key factor which is closely to the improvement of the mechanical properties of the YAG- $Al_2O_3$  composite coating dispersed with Pt particle. As the Pt particles have a good ductility, it can reduce the residual stress and the accumulated strain energy that promotes cracking and buckling at the interfaces, increase the stress tolerance and fracture toughness of bond coat. During the cyclic oxidation, when a small crack comes across the Pt particle, the Pt particle will occur to plastic deformation under tensile stress. In this process, the energy maintained the cracks propagation is absorbed by Pt particle. Then the crack is not sufficient to penetrate the Pt particle and stops propagating. So Pt particle can increase the radius of curvature of the crack tip, in other words, the crack tip is passivated. When a big crack comes across the Pt particle, Pt particles are snapped under the action of tensile stress, in the process of Pt particle occur to plastic deformation, the Pt particle will absorb most of the energy maintained the cracks propagation, when the crack tip continues to propagate to the next Pt particles, as the energy maintained the cracks propagation is significant reduced, the crack cannot penetrate Pt particle and stops propagating. Ultimately, the Pt particles can effect prevent cracks continue to propagate through the crack tip closure effect. Therefore fracture resistance of the coating can be enhanced by toughening effect of Pt particle.

Consequently, the spallation resistance of YAG- $Al_2O_3$  composite coating can be significant improved by using the following two method: one is adding PEG 20000 to the solution during the CPED process; the other is using Pt particle to toughen the coating.

## 5. Conclusion

YAG- $Al_2O_3$  composite coating dispersed with Pt particle were prepared by cathodic plasma electrolytic deposition. The coating has a special structure that the outer layer is porous and the inner layer is compact. The micropores of the coating

become smaller with the increasing of Pt particle. The thickness of the coating is up to 200 μm and it is composed of YAG, α-Al<sub>2</sub>O<sub>3</sub> and Pt particle. The current density is decreased significantly by adding PEG in solution. The cyclic oxidation tests at 1100°C demonstrate that the oxidation and spallation resistance of the YAG-Al<sub>2</sub>O<sub>3</sub>-Pt composite coatings were greatly improved with the increasing of Pt particles, due to the toughening effect of Pt particles and the effect of stress relaxation caused by porous structure. The YAG-Al<sub>2</sub>O<sub>3</sub>-Pt composite coatings possess well thermal insulation, attributed to the thermal insulation capability of YAG and the structure of vertical block micropores.

---

## References

- [1] S. B. Weber, H. L. Lein, T. Grande, M.-A. Einarsrud, Thermal and mechanical properties of crack-designed thick lanthanum zirconate coatings, *Journal of the European Ceramic Society*, 34 (2014) 975-984.
- [2] L. Pin, V. Vidal, F. Blas, F. Ansart, S. Duluard, J.-P. Bonino, Y. Le Maout, P. Lours, Optimized sol-gel thermal barrier coatings for long-term cyclic oxidation life, *Journal of the European Ceramic Society*, 34 (2014) 961-974.
- [3] R. Ghasemi, R. Shoja-Razavi, R. Mozafarinia, H. Jamali, The influence of laser treatment on thermal shock resistance of plasma-sprayed nanostructured yttria stabilized zirconia thermal barrier coatings, *Ceramics International*, 40 (2014) 347-355.
- [4] X. Zhou, Z. Xu, R. Mu, L. He, G. Huang, X. Cao, Thermal barrier coatings with a double-layer bond coat on Ni<sub>3</sub>Al based single-crystal superalloy, *Journal of Alloys and Compounds*, 591 (2014) 41-51.
- [5] N. P. Padture, M. Gell, E. H. Jordan, Thermal barrier coatings for gas-turbine engine applications, *Science*, 296 (2002) 280-284.
- [6] C. Ren, Y. D. He, D. R. Wang, Preparation and characteristics of three-layer YSZ-(YSZ/Al<sub>2</sub>O<sub>3</sub>)-YSZ TBCs, *Appl. Surf. Sci.*, 257 (2011) 6837-6842.
- [7] M. R. Brickey, J. L. Lee, Structural and Chemical Analyses of a Thermally Grown Oxide Scale in Thermal Barrier Coatings Containing a Platinum-Nickel-Aluminide Bondcoat, *Oxidation of Metals*, 54 (2000) 237-254.
- [8] G. Shanmugavelayutham, A. Kobayashi, Mechanical properties and oxidation behaviour of plasma sprayed functionally graded zirconia-alumina thermal barrier coatings, *Materials Chemistry and Physics*, 103 (2007) 283-289.
- [9] J. Y. Li, H. Dai, X. H. Zhong, Y. F. Zhang, X. F. Ma, J. Meng, X. Q. Cao, Effect of the addition of YAG (Y<sub>3</sub>Al<sub>5</sub>O<sub>12</sub>) nanopowder on the mechanical properties of lanthanum zirconate, *Materials Science and Engineering: A*, 460-461 (2007) 504-508.
- [10] H. E. Yedong, G. A. O. Wei, Theoretical consideration on composite oxide scales and coatings, *Journal of Rare Earths*, 31 (2013) 435-440.
- [11] J. Yao, Y. He, D. Wang, J. Lin, High-temperature oxidation resistance of (Al<sub>2</sub>O<sub>3</sub>-Y<sub>2</sub>O<sub>3</sub>)/(Y<sub>2</sub>O<sub>3</sub>-stabilized ZrO<sub>2</sub>) laminated coating on 8Nb-TiAl alloy prepared by a novel spray pyrolysis, *Corros. Sci.*, 80 (2014) 19-27.
- [12] J. Müller, D. Neuschütz, Efficiency of α-alumina as diffusion barrier between bond coat and bulk material of gas turbine blades, *Vacuum*, 71 (2003) 247-251.
- [13] X. Ma, Y. He, D. Wang, Preparation and high-temperature properties of Au nano-particles doped α-Al<sub>2</sub>O<sub>3</sub> composite coating on TiAl-based alloy, *Appl. Surf. Sci.*, 257 (2011) 10273-10281.
- [14] A. Keyvani, M. Saremi, M. H. Sohi, Oxidation resistance of YSZ-alumina composites compared to normal YSZ TBC coatings at 1100°C, *Journal of Alloys and Compounds*, 509 (2011) 8370-8377.
- [15] H. Lau, Influence of yttria on the cyclic lifetime of YSZ TBC deposited on EB-PVD NiCoCrAlY bondcoats and its contribution to a modified TBC adhesion mechanism, *Surf. Coat. Technol.*, 235 (2013) 121-126.
- [16] A. L. Yerokhin, X. Nie, A. Leyland, A. Matthews, S. J. Dowey, Plasma electrolysis for surface engineering, *Surf. Coat. Technol.*, 122 (1999) 73-93.
- [17] X. Yang, Y. He, D. Wang, W. Gao, Cathodic Micro-Arc Electrodeposition of Thick Ceramic Coatings, *Electrochemical and Solid-State Letters*, 5 (2002) C33.
- [18] E. Bahadori, S. Javadpour, M. H. Shariat, F. Mahzoon, Preparation and properties of ceramic Al<sub>2</sub>O<sub>3</sub> coating as TBCs on MCrAlY layer applied on Inconel alloy by cathodic plasma electrolytic deposition, *Surf. Coat. Technol.*, 228 (2013) S611-S614.
- [19] P. Wang, Y. He, J. Zhang, Al<sub>2</sub>O<sub>3</sub>-ZrO<sub>2</sub>-Pt composite coatings prepared by cathode plasma electrolytic deposition on the TiAl alloy, *Surf. Coat. Technol.*, 283 (2015) 37-43.
- [20] C. Wagner, Theoretical analysis of the diffusion processes determining the oxidation rate of alloys, *Journal of the Electrochemical Society*, 99 (1952) 369-380.
- [21] C. Wagner, Formation of composite scales consisting of oxides of different metals, *Journal of the Electrochemical Society*, 103 (1956) 627-633.